A Novel Design Method for Unequal Coupled Line Dual-Band Wilkinson Power Divider

Puria Salami[1, *], Mohsen Katebi Jahromi[2], and Alireza Khoddam Astaneh Hossein[2]

Abstract—In this article, a new design approach for an unequal coupled transmission line dual-band Wilkinson power divider is presented. A parallel short or open circuit stub is considered at the input port for dual frequency response, and two resistors are connected in order to isolate the outputs. The method is based on an even-odd mode procedure. The main objective of this paper is to fabricate a dual band Wilkinson power divider in order to achieve higher dividing ratio, simple structure, and easier fabrication. First, the desired power divider is divided to two parts known as even and odd mode equivalent circuits. Then by analyzing the circuits, the characteristic impedances are calculated. Next, the coupled transmission lines dimensions are extracted. Afterward by using the calculated characteristic impedances, an error function is formulated, and by minimizing, the isolating resistors are obtained. To clarify the applicability of this method, several microstrip power dividers which operate at both 1 GHz and 2.3 GHz with dividing ratio equal to 1.2589 are designed and simulated with the assumption that relative permittivity is equal to 2.56. In order to demonstration the advantage of using coupled lines tow dividers, one by separated-lines and the other one by coupled-lines are designed and compared with each other. The results illustrate that while the coupled-line dividers have simpler structure, they have significantly similar frequency operation to separated-line ones. Then the designed structure fabricated on an FR4 substrate and S parameters are measured. The results show excellent agreement with simulation.

1. INTRODUCTION

Wilkinson power dividers (WPDs) are widely used in microwave and millimeter-wave systems such as antenna arrays, amplifiers, and mixers. Since the invention of WPDs (Wilkinson, 1960) [1], there have been many efforts to develop them, and each tries to add additional options or introduces the most simplified approach for designing and fabricating. At first, WPDs had narrow bandwidth [2]. By using several cascade sections, the bandwidth of WPDs dramatically increased so that some nowadays WPDs have multi-gigahertz frequency response [3]. Another application was introduced by the emergence of multi-band systems, and dual-band WPDs (DWPDs) were invented [4, 5] which mostly use one or more stubs (shorted or opened circuit stubs) to have dual-band frequency operation [1–6]. Dual band coupled-line based power dividers were firstly introduced in 2009 [7] used for single band and equal dividing ratio. Since coupled lines have many advantages such as the potentiality of miniaturization, possibility to achieve higher characteristic impedances while the traces' width is constant in comparison to separated lines, and consequently higher dividing ratio, another important factor is widely researched [7–16]. The structure in [7] is based on two coupled lines with no stubs which are only used for equal operation. In [8] and [9], the analysis methods are based on two pairs of coupled lines used mainly for broadband power dividers. In these cases, dual band operation is a special case of these generalized power

* Corresponding author: Puria Salimi (psalimi84@yahoo.com).
[1] Department of Electrical Engineering, Iran University of Science and Technology, Tehran, Iran. [2] Department of Electrical Engineering, Safashahr Branch, Islamic Azad university, Safashahr, Iran

dividers. Another method is introduced in [10] which involves a sophisticated structure only used for miniaturization purposes. In this case, the unequal operation is not caused by coupled lines. In [11–14], the methods are introduced only for equal operations. None of the papers from [7] to [14] tries to use coupled line's unequal dividing operation potentiality. By investigation, it can be concluded that in both coupled and separated-line DWPDs the majority of the design approaches focus on miniaturizing or size reduction [17–23]. In this paper, a novel procedure for DWPD fabrication, based on coupled transmission lines and even-odd mode analysis [7, 24–27], is presented in order to catch 1- unequal dividing ratio as high as possible, another important factor which widely researched [28–34], 2- easier designing method, simple structure, and consequently simpler fabrication. At first, the desired structure is introduced and divided to even and odd mode equivalent circuits [33], illustrated in relevant figures. By analyzing these circuits, the even and odd mode characteristics impedances are obtained. Finally, the line characteristic impedances are calculated by using even and odd mode calculations. Second, to obtain the resistor values, regarded to input impedances from output ports, here port number 2, an error function is written and minimized. Third, several samples, for various dividing ratios and coupling coefficients (which indicate the coupling ratio between two coupled transmission lines), are analyzed, and the calculation results are listed in tables. In section four one sample is chosen. While its physical properties are recorded in a table, the simulated frequency responses are illustrated in some figures. Finally, for better understanding two DWPDs, one with separated transmission lines and the other one with coupled transmission lines, are designed, analyzed, simulated, and their S-parameters are compared with each other. Due to using coupled lines, it is clear that not only the desired structure has the miniaturizing potential, but also it can obtain higher dividing ratio than separated DWPDs.

2. ANALYSIS AND DESIGN METHOD

The desired DWPD structure is shown in Fig. 1 which consists of two impedance matching units, two coupled transmission lines, a parallel shorted or opened stub at the input port for dual operations, and two isolating resistors to isolate the outputs. In order to compute the coupled lines characteristic impedances, the mentioned DWPD must be analyzed in two modes, namely even and odd [3]. In this analysis method, the structure in Fig. 1 is divided to two parts known as even and odd mode structures [33], Figs. 2(a) and 2(b), respectively. The even mode structure, illustrated in Fig. 2(a), is a dual-band Wilkinson power divider itself [29]. As the resistors current in this mode is equal to zero, in ideal assumption, they can be omitted. In this case, the characteristic impedances of the section lines
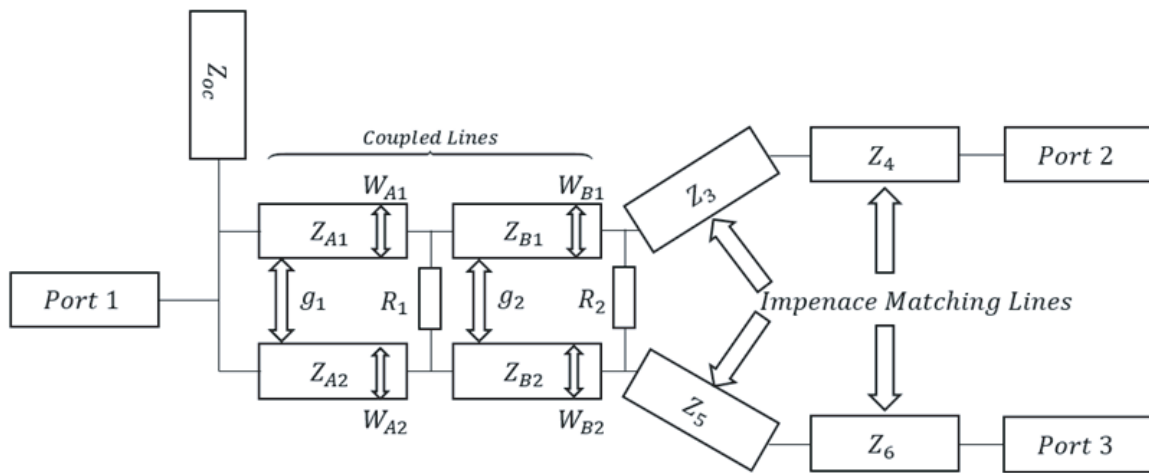
Figure 1. Dual-band coupled line Wilkinson power divider with opened stub.

(a)

(b)
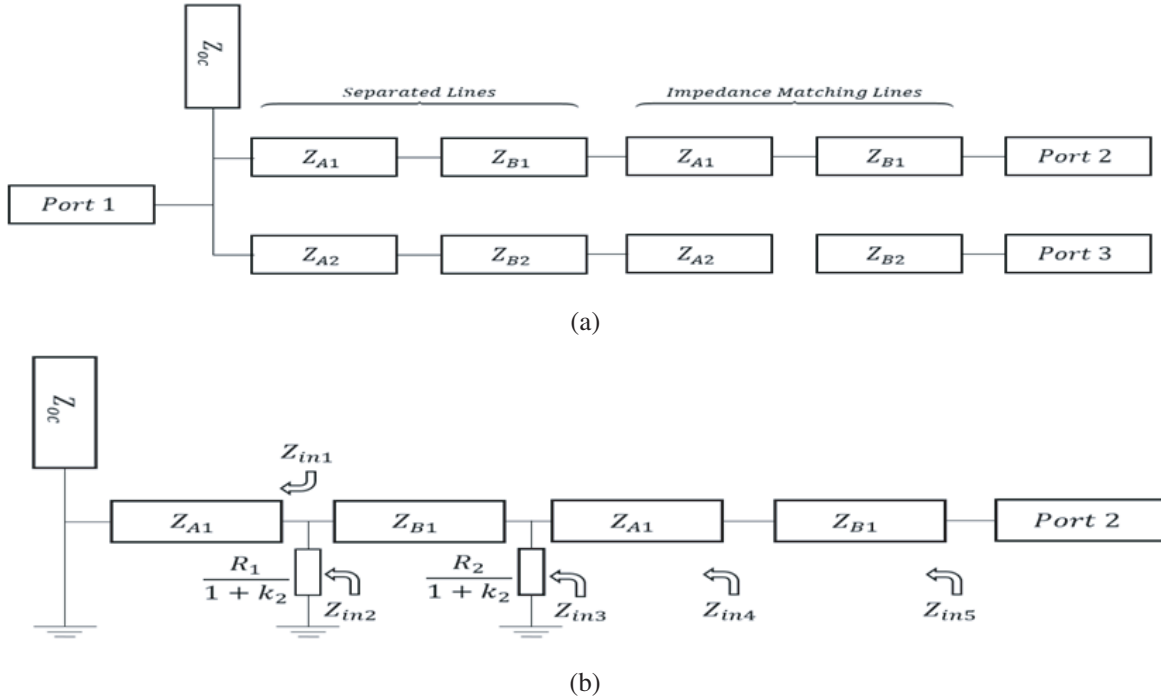
Figure 2. (a) Even mode. (b) Odd mode of the upper side of the desired DWPD.

can be obtained as follows [29]. The index e refers to even mode.

$$Z_{A1e} = \frac{\sqrt{(1+K^2)\,k}Z_0}{\tan(\theta)} \tag{1}$$

$$Z_{A2e} = \frac{\sqrt{(1+K^2)\,k}Z_0}{k^2\tan(\theta)} \tag{2}$$

$$Z_{B1e} = \sqrt{(1+K^2)\,k}Z_0\tan(\theta) \tag{3}$$

$$Z_{B2e} = \frac{\sqrt{(1+K^2)\,k}Z_0\tan(\theta)}{k^2} \tag{4}$$

where θ is the electrical length, k the dividing ratio, and Z_0 the port impedance.

For short and open stubs, the equations are as follows respectively.

$$Z_{SC} = \frac{\sqrt{k}Z_0\cos^2(\theta)}{-\cos(2\theta)\sqrt{(1+K^2)}Z_0\tan(\theta)} \tag{5}$$

$$Z_{OC} = \frac{\sqrt{k}Z_0\cos^2(\theta)\tan(2\theta)}{\cos(2\theta)\sqrt{(1+K^2)}} \tag{6}$$

Note that the electrical length of the open stub is only doubled in comparison to other lines.

In odd mode equivalent circuit, Fig. 2(b), the characteristic impedances should satisfy the followings [33].

$$k_1 = \frac{Z_{A1e} - Z_{A1o}}{Z_{A1e} + Z_{A1o}} = \frac{Z_{A2e} - Z_{A2o}}{Z_{A2e} + Z_{A2o}} \tag{7}$$

$$k_1 = \frac{Z_{B1e} - Z_{B10}}{Z_{B1e} + Z_{B1o}} = \frac{Z_{B2e} - Z_{B2o}}{Z_{B2e} + Z_{B2o}} \tag{8}$$

where k_1 is the coupling coefficient which is chosen in a way that the gaps between the coupled lines can be easily fabricated [3]. Thus, the even and odd mode impedances follow the relations bellow. The

index o refers to odd mode.

$$Z_{A10} = Z_{A1e} \left(\frac{1 - k_1}{1 + k_1} \right) \tag{9}$$

$$Z_{B1o} = Z_{B1e} \left(\frac{1 - k_1}{1 + k_1} \right) \tag{10}$$

$$Z_{A2o} = Z_{A2e} \left(\frac{1 - k_1}{1 + k_1} \right) \tag{11}$$

$$Z_{B2o} = Z_{B2e} \left(\frac{1 - k_1}{1 + k_1} \right) \tag{12}$$

By knowing the even-odd mode impedances, the line characteristic impedances can be calculated by following equations

$$Z_{A1} = \sqrt{Z_{A1e} \times Z_{A1o}} \tag{13}$$

$$Z_{B1} = \sqrt{Z_{B1e} \times Z_{B1o}} \tag{14}$$

$$Z_{A2} = \sqrt{Z_{A2e} \times Z_{A2o}} \tag{15}$$

$$Z_{B2} = \sqrt{Z_{B2e} \times Z_{B2o}} \tag{16}$$

For outputs impedance matching transmission lines, two impedance transformers are considered. To calculate their characteristic impedances, the following equations are used [29].

$$Z_3 = Z_0 \sqrt{ \frac{k}{2 \tan^2(\theta)} (1 - k) + \sqrt{ \left[\frac{k}{2 \tan^2(\theta)} (1 - k) \right]^2 + k^3 } } \tag{17}$$

$$Z_4 = \frac{Z_0 \sqrt{ \frac{k}{2 \tan^2(\theta)} (k - 1) + \sqrt{ \left[\frac{k}{2 \tan^2(\theta)} (1 - k) \right]^2 + k^3 } }}{\sqrt{k}} \tag{18}$$

$$Z_5 = \frac{z_0 \sqrt{ \frac{(k - 1)}{2 \tan^2(\theta)} + \sqrt{ \left[\frac{(1 - k)}{2 \tan^2(\theta)} \right]^2 + k } }}{k} \tag{19}$$

$$Z_6 = \frac{Z_0 \sqrt{ \frac{(1 - k)}{2 \tan^2(\theta)} + \sqrt{ \left[\frac{(1 - k)}{2 \tan^2(\theta)} \right]^2 + k } }}{\sqrt{k}} \tag{20}$$

It is obvious that since the impedance matching transmission lines are separated, Equations (17) to (20) are independent from coupling coefficient. Thus, the impedance matching transmission lines' characteristic impedances are constant while k is constant.

As the final step, the isolation resistors should be obtained. For this purpose, the odd mode equivalent circuit, Fig. 2(b), is used [33]. Here the input impedance form port 2 is considered as error function, and its calculation procedure is declared as follows.

$$Z_{in1} = jZ_{A1} \tan(\theta) \tag{21}$$

$$Z_{in2} = \frac{R_1 \times jZ_{A1} \tan(\theta)}{R_1 + jZ_{A1} \tan(\theta)} \tag{22}$$

$$Z_{in3} = Z_{B1} \frac{Z_{in2} + jZ_{B1} \tan(\theta)}{Z_{B1} + jZ_{in2} \tan(\theta)} = Z_{B1} \frac{jR_1 Z_{A1} \tan(\theta) + jZ_{B1} \tan(\theta) \left(R_1 + jZ_{A1} \tan(\theta) \right)}{Z_{B1} \left(R_1 + jZ_{A1} \tan(\theta) \right) - R_1 Z_{A1} \tan(\theta) \tan(\theta)} \tag{23}$$

$$Z_{in4} = \frac{R_2 \times Z_{in3}}{R_2 + Z_{in3}} = \frac{R_2 Z_{B1}\left(jR_1 Z_{A1}\tan(\theta) + jZ_{B1}\tan(\theta)\left(R_1 + jZ_{A1}\tan(\theta)\right)\right)}{\begin{array}{c}R_2\left(Z_{B1}\left(R_1 + jZ_{A1}\tan(\theta)\right) - R_1 Z_{A1}\tan(\theta)\tan(\theta)\right)\\ +Z_{B1}\left(jR_1 Z_{A1}\tan(\theta) + jZ_{B1}\tan(\theta)\left(R_1 + jZ_{A1}\tan(\theta)\right)\right)\end{array}} \tag{24}$$

$$
\begin{aligned}
Z_{in5} &= Z_3 \frac{Z_{in4} + jZ_3\tan(\theta)}{Z_3 + jZ_{in4}\tan(\theta)}\\[2mm]
&= Z_3 \frac{\left(\dfrac{R_2 Z_{B1}\left(jR_1 Z_{A1}\tan(\theta)+jZ_{B1}\tan(\theta)\left(R_1+jZ_{A1}\tan(\theta)\right)\right)}{\begin{array}{c}R_2\left(Z_{B1}\left(R_1+jZ_{A1}\tan(\theta)\right)-R_1 Z_{A1}\tan(\theta)\tan(\theta)\right)\\ +Z_{B1}\left(jR_1 Z_{A1}\tan(\theta)+jZ_{B1}\tan(\theta)\left(R_1+jZ_{A1}\tan(\theta)\right)\right)\end{array}}\right) + jZ_3\tan(\theta)}{Z_3 + j\left(\dfrac{R_2 Z_{B1}\left(jR_1 Z_{A1}\tan(\theta)+jZ_{B1}\tan(\theta)\left(R_1+jZ_{A1}\tan(\theta)\right)\right)}{\begin{array}{c}R_2(Z_{B1}(R_1+jZ_{A1}\tan(\theta))-R_1 Z_{A1}\tan(\theta)\tan(\theta))\\ +Z_{B1}\left(jR_1 Z_{A1}\tan(\theta)+jZ_{B1}\tan(\theta)\left(R_1+jZ_{A1}\tan(\theta)\right)\right)\end{array}}\right)\tan(\theta)}
\end{aligned}
\tag{25}
$$

$$
\begin{aligned}
Z_{in} &= Z_4 \frac{Z_{in5} + jZ_4\tan(\theta)}{Z_4 + jZ_{in5}\tan(\theta)}\\[2mm]
&= Z_4 \frac{Z_3\left(\dfrac{\dfrac{R_2 Z_{B1}\left(jR_1 Z_{A1}\tan(\theta)+jZ_{B1}\tan(\theta)\left(R_1+jZ_{A1}\tan(\theta)\right)\right)}{\begin{array}{c}R_2\left(Z_{B1}\left(R_1+jZ_{A1}\tan(\theta)\right)-R_1 Z_{A1}\tan(\theta)\tan(\theta)\right)\\ +Z_{B1}\left(jR_1 Z_{A1}\tan(\theta)+jZ_{B1}\tan(\theta)\left(R_1+jZ_{A1}\tan(\theta)\right)\right)\end{array}} + jZ_3\tan(\theta)}{Z_3 + j\dfrac{R_2 Z_{B1}\left(jR_1 Z_{A1}\tan(\theta)+jZ_{B1}\tan(\theta)\left(R_1+jZ_{A1}\tan(\theta)\right)\right)}{\begin{array}{c}R_2\left(Z_{B1}\left(R_1+jZ_{A1}\tan(\theta)\right)-R_1 Z_{A1}\tan(\theta)\tan(\theta)\right)\\ +Z_{B1}\left(jR_1 Z_{A1}\tan(\theta)+jZ_{B1}\tan(\theta)\left(R_1+jZ_{A1}\tan(\theta)\right)\right)\end{array}}\tan(\theta)}\right) + jZ_4\tan(\theta)}{Z_4 + jZ_3\left(\dfrac{\dfrac{R_2 Z_{B1}\left(jR_1 Z_{A1}\tan(\theta)+jZ_{B1}\tan(\theta)\left(R_1+jZ_{A1}\tan(\theta)\right)\right)}{\begin{array}{c}R_2\left(Z_{B1}\left(R_1+jZ_{A1}\tan(\theta)\right)-R_1 Z_{A1}\tan(\theta)\tan(\theta)\right)\\ +Z_{B1}\left(jR_1 Z_{A1}\tan(\theta)+jZ_{B1}\tan(\theta)\left(R_1+jZ_{A1}\tan(\theta)\right)\right)\end{array}} + jZ_3\tan(\theta)}{Z_3 + j\dfrac{R_2 Z_{B1}\left(jR_1 Z_{A1}\tan(\theta)+jZ_{B1}\tan(\theta)\left(R_1+jZ_{A1}\tan(\theta)\right)\right)}{\begin{array}{c}R_2\left(Z_{B1}\left(R_1+jZ_{A1}\tan(\theta)\right)-R_1 Z_{A1}\tan(\theta)\tan(\theta)\right)\\ +Z_{B1}\left(jR_1 Z_{A1}\tan(\theta)+jZ_{B1}\tan(\theta)\left(R_1+jZ_{A1}\tan(\theta)\right)\right)\end{array}}\tan(\theta)}\right)\tan(\theta)}
\end{aligned}
\tag{26}
$$

The final formula is considered as an error function. As seen, the error function, (Z_{in}), is a function of R_1 and R_2. On the other hand, the only uncalculated variables are these mentioned resistors. Hence by minimizing this function, the resistor values will be calculated. Note that Z_{in} must be equal to port 2 impedance (here $50\,\Omega$).

3. EXAMPLES AND SIMULATION

In this section, several examples of a DWPD whit open stub, based on an FR4 layout ($\varepsilon_r = 4.47$) for various dividing ratios, ideal transmission lines, $f_1 = 1$, $f_1 = 2.3$, and port impedances equal to $50\,\Omega$ are analyzed. The calculated parameters are listed in Tables 1 and 2. It is obvious from Table 2 that the more increase is in coupling factor, k_1, the more decrease is in lines characteristic impedances. For simulation, case number 8 is chosen, and the frequency responses are illustrated in Figs. 3 to 5. In this case, a program based on equations in [34] has been written in MATLAB to calculate the even-odd mode characteristic impedances for wide range of trace widths and various coupling factors in order to build a physical matrix. Then by using another MATLAB program, the final physical dimensions are extracted, using interpolation within the mentioned matrix. The physical dimensions, in millimeters, are listed in Table 3 where W_{A_1} is the trace width corresponding to Z_{A_1}, etc. The final structure is shown in Figs. 6 and 7. It can be observed that this structure not only is very simple but also has good division and isolation within output ports and excellent matching in all ports through desired frequency bands.

Figure 3 shows S_{12} and S_{13}, the delivered power to port 2 and port 3, respectively. As can be

Table 1. Even-Odd Mode Results.

case	k	f_1	f_2	c	Z_{A1e}	Z_{B1e}	Z_{A2e}	Z_{B2e}	Z_{A1o}	Z_{B1o}	Z_{A2o}	Z_{B2o}
1	1:1	1	2.3	0	50.35	99.29	50.35	99.29	50.35	99.29	50.35	99.29
2	1:1.2589	1	2.3	0	64.22	126.66	40.52	79.92	64.22	126.66	40.52	79.92
3	1:1.7	1	2.3	0	112.59	222.03	28.14	55.51	91.56	180.56	31.68	62.47
4	1:1	1	2.3	0.16	50.35	99.29	50.35	99.29	36.46	71.9	36.46	71.9
5	1:1.2589	1	2.3	0.16	64.22	126.66	40.52	79.92	46.5	91.72	29.34	57.87
6	1:1.7	1	2.3	0.16	112.59	222.03	28.14	55.51	66.3	130.75	22.94	40.19
7	1:1	1	2.3	0.27	50.35	99.29	50.35	99.29	28.94	57.07	28.94	57.07
8	**1:1.2589**	**1**	**2.3**	**0.27**	**64.22**	**126.66**	**40.52**	**79.92**	**36.91**	**72.8**	**23.29**	**45.93**
9	1:1.7	1	2.3	0.27	112.59	222.03	28.14	55.51	52.62	103.78	18.21	35.91

Table 2. The Lines' Characteristic Impedances.

| case	k	c	Z_0	Z_{A1}	Z_{B1}	Z_{A2}	Z_{B2}	Z_3	Z_4	Z_5	Z_6	Z_{oc}
1	1:1	0	50	50.35	99.29	50.35	99.29	50	50	50	50	105.08
2	1:1.2589	0	50	64.22	126.66	40.52	79.92	57.71	54.53	43.31	45.84	**103.71**
3	1:1.7	0	50	91.56	180.56	31.68	62.47	69.55	61.1	35.94	40.91	98.24
4	1:1	0.16	50	42.84	84.5	42.84	84.5	50	50	50	50	105.08
5	1:1.2589	0.16	50	54.65	107.78	34.48	68.0	57.71	54.53	43.31	45.84	**103.71**
6	1:1.7	0.16	50	77.91	153.65	26.96	53.16	69.55	61.1	35.94	40.91	98.24
7	1:1	0.27	50	38.17	75.28	37.17	75.28	50	50	50	50	105.08
8	**1:1.2589**	**0.27**	**50**	**48.69**	**96.028**	**30.72**	**60.59**	**57.71**	**54.53**	**43.31**	**45.84**	**103.71**
9	1:1.7	0.27	50	69.41	136.89	2401	47.36	69.55	61.1	35.94	40.91	98.24
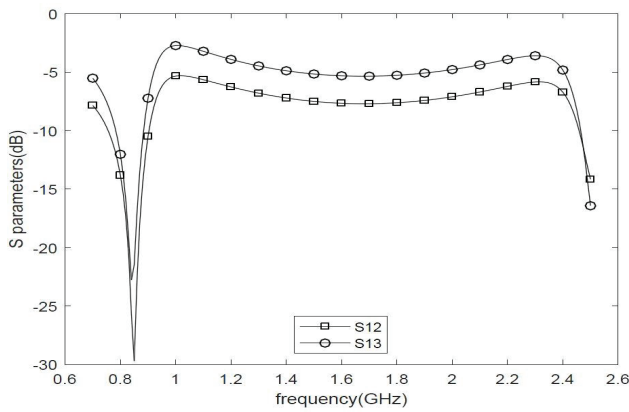
Figure 3. Outputs S-parameters.
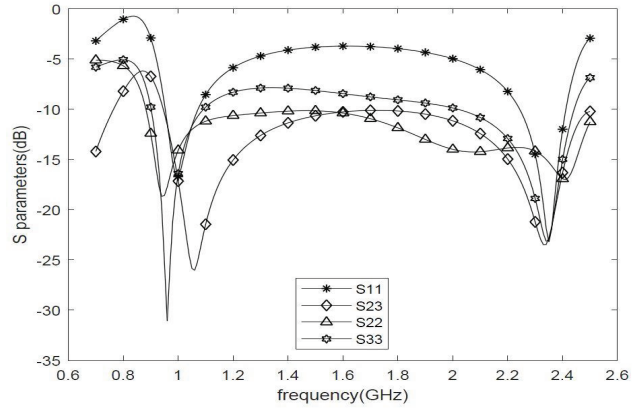
Figure 4. Reflection losses and Outputs isolation and matching: S_{11} is input reflection, S_{23} is outputs isolation, S_{22} and S_{33} are outputs matching.
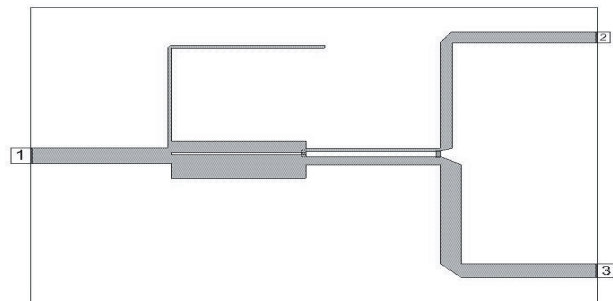
Table 3. Physical Dimensions for Case Number 8.

| | | | $\varepsilon_r = 4.47$ | | $h = 1.6$ mm | | $f_1 = 1$ GHz | | $f_2 = 2.3$ GHz | | | |
| | | | coupled factor $(k_1) = 0.16$ | | | | port impedances = 50 Ω | | | | | |
W_{A_1}	W_{B_1}	W_{A_2}	W_{B_2}	W_3	W_4	W_5	W_6	W_{oc}	g_1(mm)	g_2(mm)	$R_1\,\Omega$	$R_2\,\Omega$
2.66	0.626	5.56	1.9	2.2	2.5	3.7	3.3	0.57	0.6	1.3	81	160
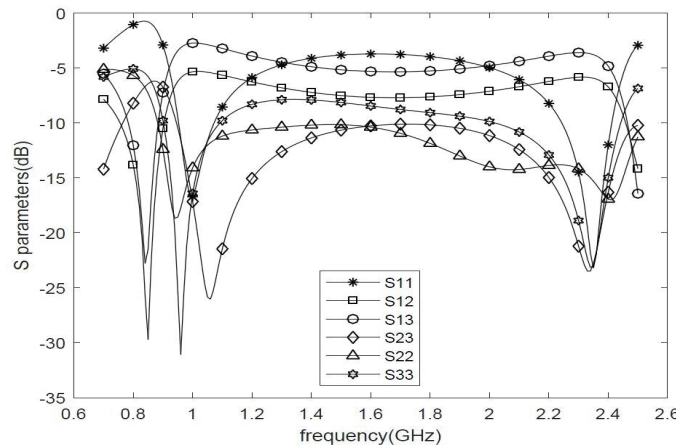
Figure 5. S-parameters.
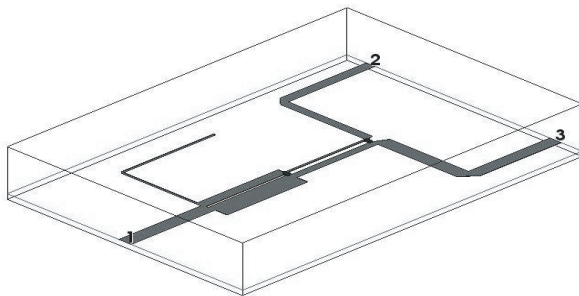
Figure 6. 3D physical structure.

Figure 7. Physical structure.

seen, the division between two output ports within desired frequencies is reasonably constant, -5.3 dB and -5.9 dB for S_{12}, -2.8 dB and -3.5 dB for S_{13} in frequencies 1 and 2.3 GHz, respectively. At the same time, the reflection at all ports (S_{11}, S_{22}, and S_{33}) and the isolation between two outputs (S_{23}) are far below -10 dB which indicate excellent port matching and output isolation, Fig. 4. For better understanding the S_{12}, S_{13}, ports matching and isolation are shown against each other in Fig. 5.

4. COMPARISON

In this section, by some comparisons, we are going to describe how this design approach helps to achieve two desired purposes. Looking at Figs. 6, 7, and 8(a), it is obvious that the coupled transmission lines are straight and have the same length, while the separated transmission lines have different lengths and have to be fabricated separately, Fig. 8(b). Thus, there are many uses of curves and bends. Consequently, the separated structure has some limitations that constrain the fabrication which are dramatically decreased by replacing separated lines with couple lines. On the other hand, while the dividing ratio increases, the transmission lines' width decreases in a way that from a certain dividing ratio, depending on substrate,
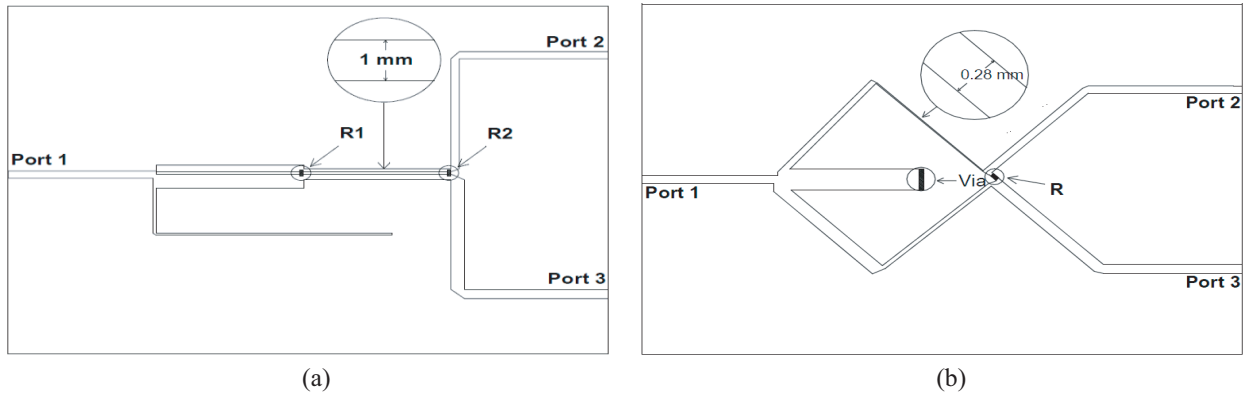
Figure 8. Comparison between two structures: (a) coupled-line DWPD structure, (b) separated-line DWPD structure.
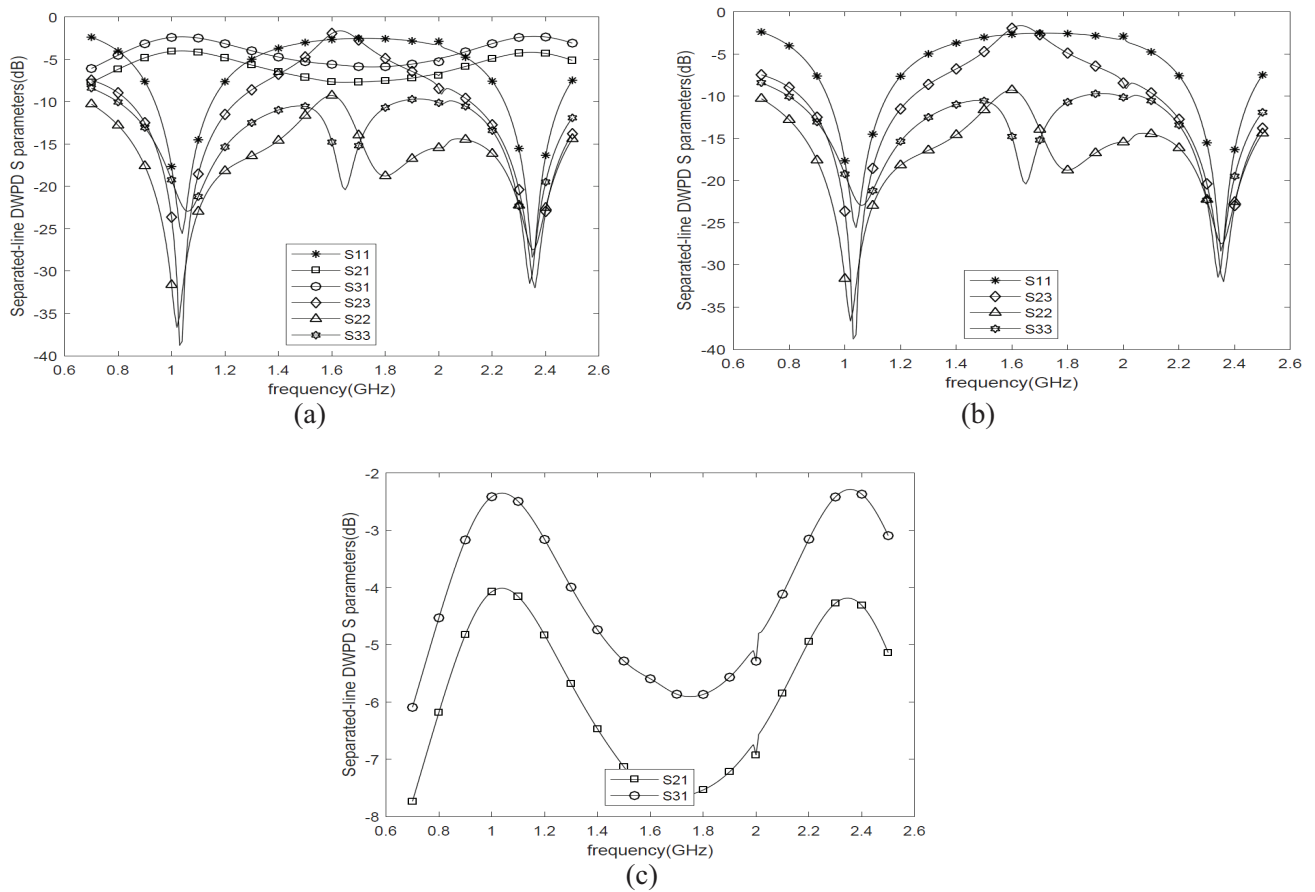
Figure 9. Frequency responses of separated line DWPD shown in Fig. 8(a): (a) divided parameters against ports' impedance matching and output isolation, (b) ports' impedance matching and output isolation, (c) divided parameters.

some lines become too narrow so that the fabrication will be impossible physically. For describing the second purpose, achieving the higher dividing ratio, there are two DWPDs, coupled-line and separated-line DWPDs, with $k = 1.2589$ [29] designed and simulated on an F4B substrate with 0.8 mm thickness
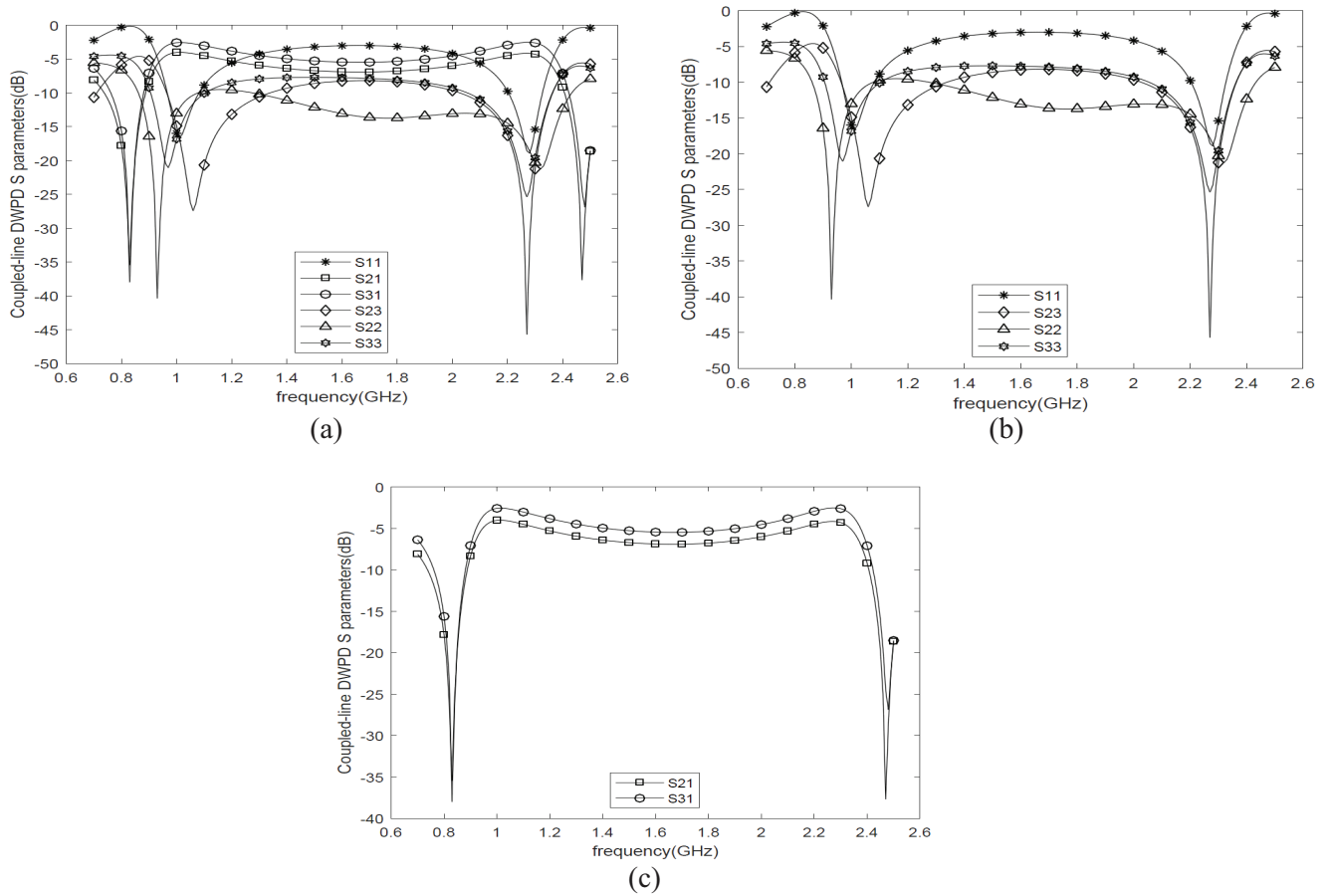
Figure 10. Frequency responses of coupled line DWPD shown in Fig. 8(b), (a) divided parameters against ports' impedance matching and output isolation, (b) ports' impedance matching and output isolation, (c) divided parameters.

Table 4. Physical dimensions for separated-line DWPD fabricated on F4B.

|			$\varepsilon_r = 2.65$	$h = 0.8$ mm		$f_1 = 1$ GHz	$f_2 = 2.3$ GHz					
			coupled factor $(k_1) = 0$			port impedances = 50 Ω						
	W_{A_1}	W_{B_1}	W_{A_2}	W_{B_2}	W_3	W_4	W_5	W_6	W_{oc}	g_1(mm)	g_2(mm)	$R_1 \Omega$
separated	1.41	0.28	2.9	0.93	1.7	1.9	2.7	2.5	0.57	>3	>3	68

Table 5. Physical dimensions for coupled-line DWPD fabricated on F4B.

|			$\varepsilon_r = 2.65$	$h = 0.8$ mm		$f_1 = 1$ GHz	$f_2 = 2.3$ GHz						
			coupled factor $(k_1) = 0.16$			port impedances = 50 Ω							
	W_{A_1}	W_{B_1}	W_{A_2}	W_{B_2}	W_3	W_4	W_5	W_6	W_{oc}	g_1(mm)	g_2(mm)	$R_1 \Omega$	$R_2 \Omega$
coupled	1.9	1	3.8	1.9	1.7	1.9	2.7	2.5	0.57	0.6	0.6	68	120

and 2.65 relative permittivity in HFSS software, and their dimensions are listed in Tables 4 and 5. By comparing them respectively, it is derived that while the operations of these two dividers are reasonably similar, using coupled lines reduces physical fabrication limitations since all traces in coupled lines are wider than the other transmission lines respectively. The main important dimension more responsible
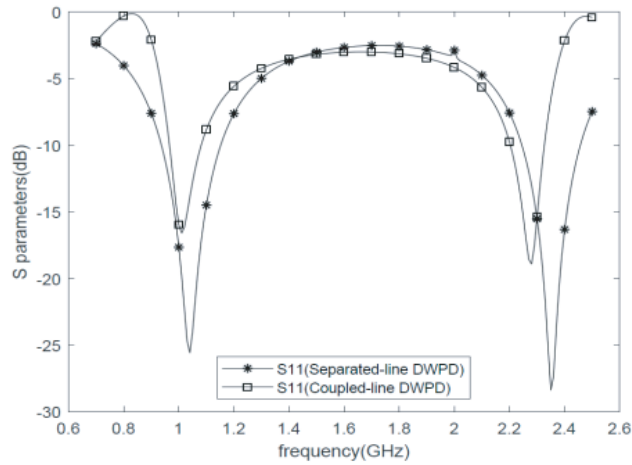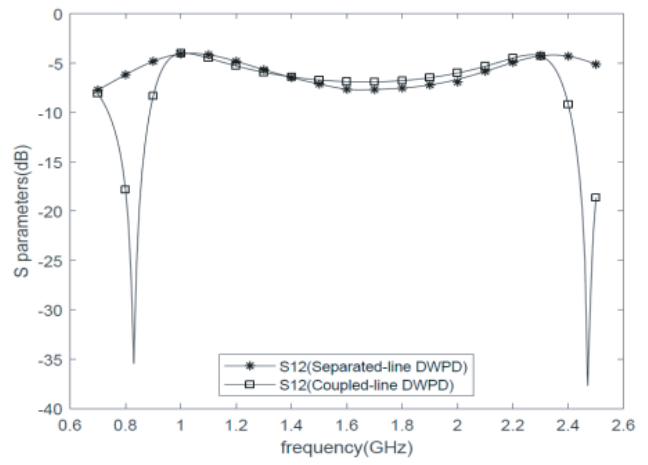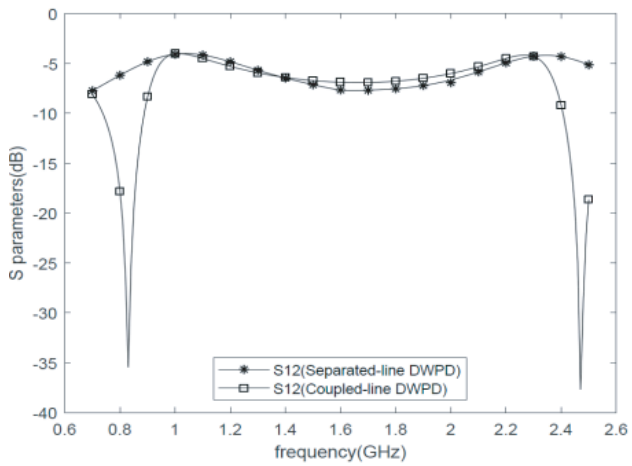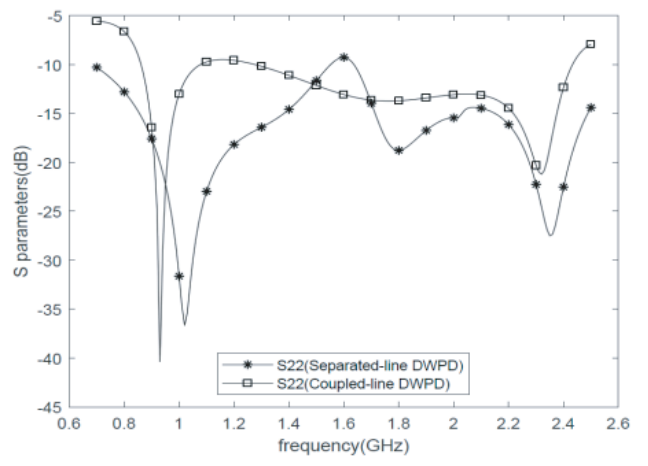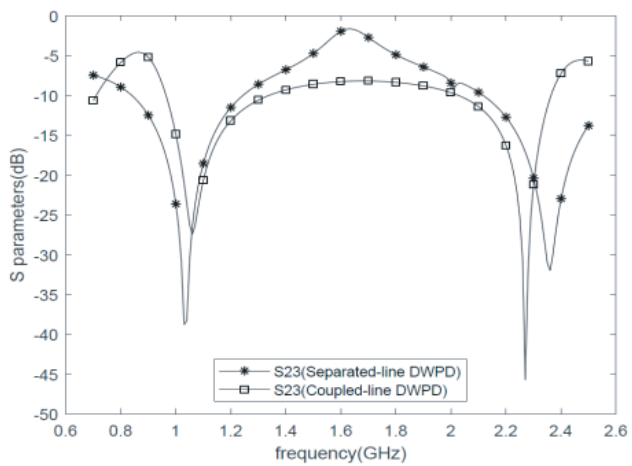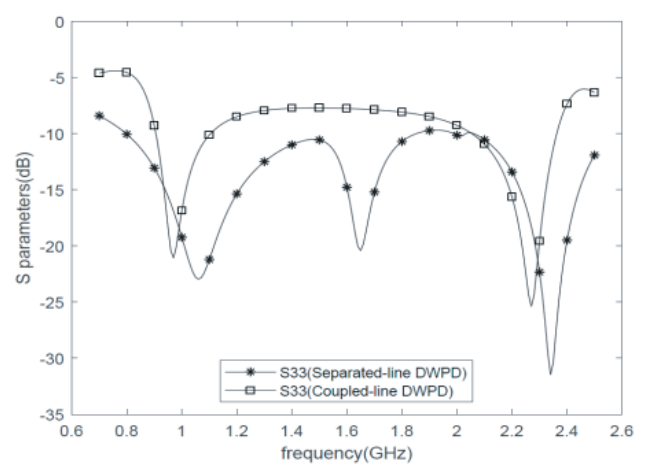
Figure 11. The separated-line and coupled-lines DWPD S-parameters comparison against each other separately: (a) S_{11} comparison, (b) S_{12} comparison, (a) S_{13} comparison, (d) S_{23} comparison, (e) S_{22} comparison, (f) S_{33} comparison.

for physical limitation is W_{B_1} which is 0.28 mm in separated-line DWPD, Fig. 8(b), while the same value in Fig. 8(a) is 1 mm, more than tripled. This fact reduces the fundamental DWPDs physical limitation. To clarify the operation similarity, both designed DWDPs are simulated, and their frequency responses are demonstrated in Figs. 9 and 10 and compared in Fig. 11.

Fig. 9(a) represents the separated line DWPD S parameters while its corresponding S parameters for coupled line DWPD is in Fig. 10(a). For better understanding we separated impedance matching and isolating parameters from dividing ones and prepared Figs. 9(b) and 9(c) and also Figs. 10(b) and 10(c). By an overview, it can be concluded that coupled-line and separated-line DWPDs have the same S parameters. Figs. 9(b) and 10(b) illustrate reflection loss and matching at all ports. As it is seen, these parameters are reasonably similar, far below -10 dB, at desired frequencies. In Fig. 9(c) at frequency 1 GHz, the delivered powers to ports 2 and 3 in separate-line DWDP are -4.07 dB and -2.41 dB while these values are -4.27 dB and -2.41 dB at 2.3 GHz, respectively. On the other hand, in Fig. 10(c) at frequency 1 GHz, the delivered powers to port 2 and 3 in coupled-line DWDP are -4.03 dB and -2.58 dB while these values are -4.29 dB and -2.61 dB at 2.3 GHz, respectively. It is clear that the delivered powers to outputs are not only significantly equal, but also in desired frequencies, and the coupled-line WDPW operates the same as the separated-line WDPW but with wider transmission lines.

The separate S parameter comparisons are illustrated in Fig. 11. In Figs. 11(a), (d), (f), impedance matching in ports 1, 2, and 3 is presented respectively. These parameters have the same behavior due to having the value far below -10 dB in both 1 and 2.3 GHz frequencies. At the same time, Figs. 9(b) and (c) demonstrate S_{21} and S_{31} comparison. It is clear that both mentioned parameters have exactly the same value in 1 and 2.3 GHz frequencies. Consequently, the separated and coupled DWPDs have excellent agreement in desired frequencies.

Now we are going to explain that how much higher dividing ratio can be achieved after using coupled transmission lines while the W_{B_1} width is constant and equal to what is listed in Table 4. As Table 6 demonstrates, although W_{B_1} in both separated and coupled line DWPDs are equal, the dividing ratio in coupled structure is higher than that in separated one about 0.5. In conclusion, it means that

**Table 6.** Physical dimensions for coupled-line DWPD fabricated on F4B.

|	$\varepsilon_r = 2.65$			$h = 0.8$ mm			$f_1 = 1$ GHz	$f_2 = 2.3$ GHz						
				coupled factor (k_1) is 0.16 for coupled and is 0 for separated one										
	k	W_{A_1}	W_{B_1}	W_{A_2}	W_{B_2}	W_3	W_4	W_5	W_6	W_{oc}	g_1(mm)	g_2(mm)	$R_1\,\Omega$	$R_2\,\Omega$
separated	1.2	1.41	0.28	2.9	0.93	1.7	1.9	2.7	2.5	0.5	>3	>3	68	-
coupled	1.7	1.30	0.28	5.46	2.26	1.7	1.9	2.7	2.5	0.5	0.6	0.6	68	120
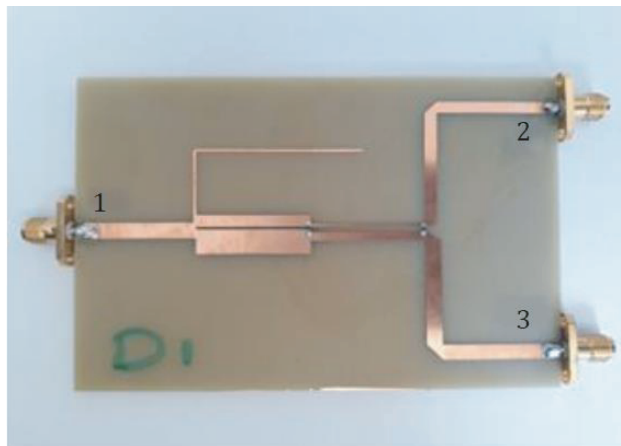
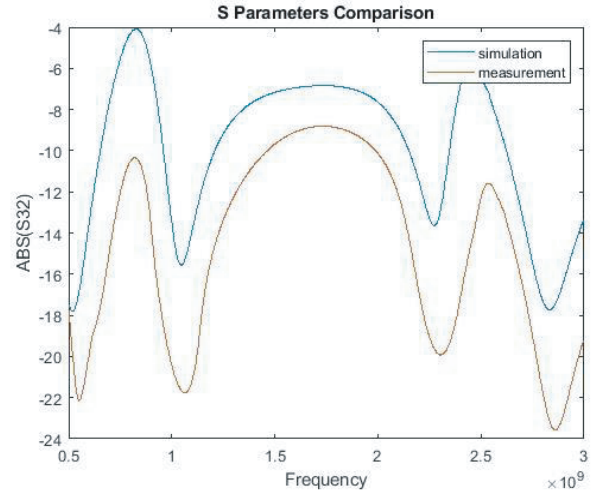**Figure 12.** The fabricated circuit on FR4 substrate.
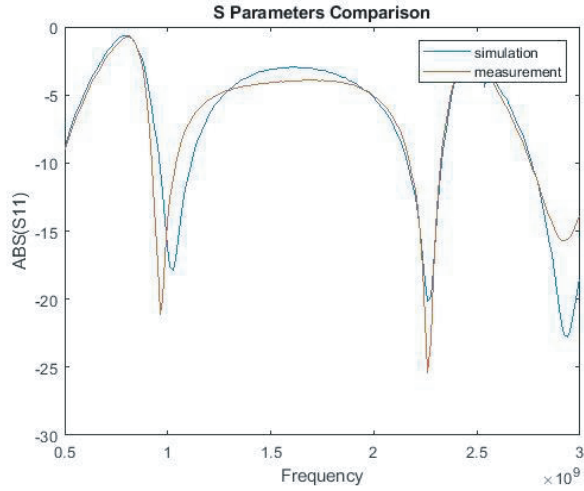
Figure 13. Measured and simulation S_{11} comparison.
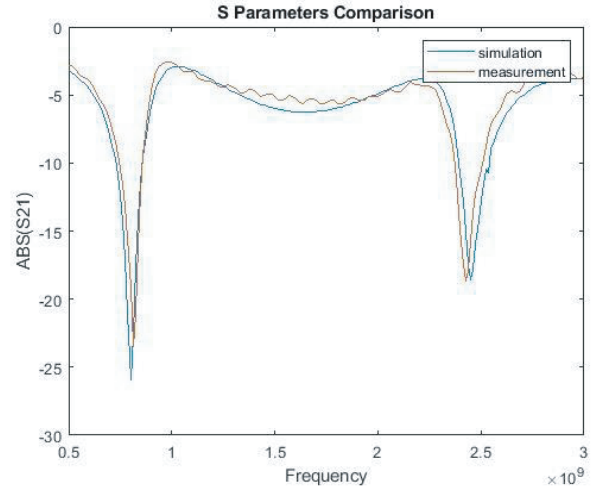
Figure 14. Measured and simulation S_{12} comparison.
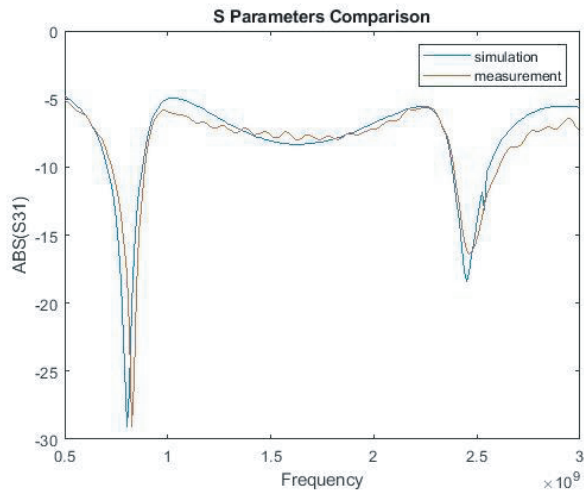
Figure 15. Measured and simulation S_{31} comparison.

Figure 16. Measured and simulation S_{32} comparison.

the coupled line DWPDs with higher dividing ratio can be designed and fabricated easier than separated line DWPDs.

5. RESULTS AND DISCUSSION

Figures 12 shows the fabricated circuit on an FR4 substrate with ε equal to 4.4 and thickness of 1.6 mm. The scattering parameters of the designed power divider have been measured. Fig. 13 to Fig. 16 show the simulated and measured scattering parameters of the fabricated power divider simultaneously. Fig. 13 shows the magnitude of the reflection coefficient at port 1. As the figure shows, the magnitude of the measured reflection coefficient has excellent agreement with simulated one and has its lowest values in 1 and 2.2 GHz frequencies. Figs. 14 and 15 show the magnitude of the reflection coefficient at port 2 and port 3, respectively. As it is seen, measured and simulated parameters follow each other excellently. There is some ripple on the measured curves due to laboratory situation. Fig. 16 illustrates the measured and simulated isolation comparison between the output ports. The two curves have the same look with a slight deference which is negligible.

6. CONCLUSION

In this article, a new structure for a dual-band Wilkinson power divider, based on coupled microstrip transmission lines is introduced. The mentioned Wilkinson power divider is divided to even and odd mode equivalent circuits, then their relevant characteristics are calculated. Due to matching purpose, two matching units are considered and calculated. By using odd mode circuit, an error function is written, and by minimization the resistor values are obtained. For analysis, several samples are analyzed, and the corresponding calculated parameters are listed in two tables. To clarify the applicability, an example is chosen, fabricated on an FR4 substrate and simulated in microwave office software. The measured and simulated S-parameters show excellent frequency response within desired band. Note that his method can be used for separated transmission lines when coupling factor is equal to zero, so in final section two DWPDs, one by separated transmission lines while the other by coupled transmission lines, are analyzed and compared. Consequently, the comparison reveals that the desired DWPDs have the potential to operate reasonably the same as the separated DWPDs while they have wider traces. This fact means significant reduction of the fabricating limitation in higher dividing ratios.

REFERENCES

1. Wilkinson, E. J., "An N-way hybrid power divider," *IRE Transactions on Microwave Theory and Techniques*, Vol. 8, No. 1, 116–118, 1960.
2. Pozar, D. M., *Microwave Engineering*, Johnwiley & Sons. Inc., 367–368, New York, 1998.
3. Salimi, P., M. Moradianpour, and E. Borzabadi, "Broadband asymmetrical multi-section coupled line Wilkinson power divider with unequal power dividing ratio," *Progress In Electromagnetics Research C*, Vol. 43, 217–229, 2013.
4. Lin, I.-H., M. DeVincentis, C. Caloz, et al., "Arbitrary dual-band components using composite right/left-handed transmission lines," *IEEE Transactions on Microwave Theory and Techniques*, Vol. 52, No. 4, 1142–1149, 2004.
5. Wu, L., H. Yilmaz, T. Bitzer, et al., "A dual-frequency Wilkinson power divider: For a frequency and its first harmonic," *IEEE Microwave and Wireless Components Letters*, Vol. 15, No. 2, 107–109, 2005.
6. Wu, Y., Y. Liu, Y. Zhang, et al., "A dual band unequal Wilkinson power divider without reactive components," *IEEE Transactions on Microwave Theory and Techniques*, Vol. 57, No. 1, 216–222, 2008.
7. Park, M.-J., "Two-section cascaded coupled line Wilkinson power divider for dual-band applications," *IEEE Microwave and Wireless Components Letters*, Vol. 19, No. 4, 188–190, 2009.
8. Wu, Y., Y. Liu, and Q. Xue, "An analytical approach for a novel coupled-line dual-band Wilkinson power divider," *IEEE Transactions on Microwave Theory and Techniques*, Vol. 59, No. 2, 286–294, 2010.
9. Li, J., Y. Wu, Y. Liu, J.-Y. Shen, S. Li, and C. Yu, "A generalized coupled-line dual-band Wilkinson power divider with extended ports," *Progress In Electromagnetics Research*, Vol. 129, 197–214, 2012.
10. Wang, X., I. Sakagami, A. Mase, et al., "Dual-band Wilkinson power divider and its miniaturization using coupled line sections," *2012 Asia Pacific Microwave Conference Proceedings*, 1256–1258, IEEE, 2012.
11. Tsai, G.-D. and Y.-H. Pang, "Dual-band Wilkinson power divider using cross-paired coupled lines," *2012 Asia Pacific Microwave Conference Proceedings*, 980–982, IEEE, 2012.
12. Wang, W. M. and Y. A. Liu, "A novel small-size coupled-line Wilkinson power divider for dual-band applications," *Applied Mechanics and Materials*, Vol. 437, 1066–1072, 2013.
13. Xu, X. and X. Tang, "A design approach for dual-band Wilkinson power divider with two pairs of coupled-line sections," *Progress In Electromagnetics Research Letters*, Vol. 45, 81–87, 2014.

14. Maktoomi, M. H., D. Banerjee, and M. S. Hashmi, "An enhanced frequency-ratio coupled-line dual-frequency Wilkinson power divider," *IEEE Transactions on Circuits and Systems II: Express Briefs*, Vol. 65, No. 7, 888–892, 2017.

15. Ravelo, B. and O. Maurice, "Kron-Branin modeling of YY-tree interconnects for the PCB signal integrity analysis," *IEEE Transactions on Electromagnetic Compatibility*, Vol. 59, No. 2, 411–419, 2016.

16. Ravelo, B., O. Maurice, and S. Lalléchère, "Asymmetrical 1: 2 Y-tree interconnects modelling with Kron-Branin formalism," *Electronics Letters*, Vol. 52, No. 14, 1215–1216, 2016.

17. Kumar, A. and N. P. Pathak, "A compact reconfigurable concurrent dual-band Wilkinson power divider for noninvasive vital sign detection applications," *2014 International Conference on Signal Propagation and Computer Technology (ICSPCT 2014)*, 434–437, IEEE, 2014.

18. Mohra, A. S., "Compact dual band Wilkinson power divider," *Microwave and Optical Technology Letters*, Vol. 50, No. 6, 1678–1682, 2008.

19. Rostami, P. and S. Roshani, "A miniaturized dual band Wilkinson power divider using capacitor loaded transmission lines," *AEU-International Journal of Electronics and Communications*, Vol. 90, 63–68, 2018.

20. Wang, X., N. Kimata, Z. Ma, et al., "Dual-band bandpass filter type Wilkinson power divider with microstrip composite resonators," *2017 IEEE Asia Pacific Microwave Conference (APMC)*, 299–301, IEEE, 2017.

21. Wang, X., I. Sakagami, Z. Ma, et al., "Generalized, miniaturized, dual-band Wilkinson power divider with a parallel RLC circuit," *AEU-International Journal of Electronics and Communications*, Vol. 69, No. 1, 418–423, 2015.

22. Wang, Z., J. S. Jang, and C.-W. Park, "Compact dual-band Wilkinson power divider using lumped component resonators and open-circuited stubs," *WAMICON 2011 Conference Proceedings*, 1–4, IEEE, 2011.

23. Wu, Y., Y. A. Liu, and S. Li, "A compact pi-structure dual band transformer," *Progress In Electromagnetics Research*, Vol. 88, 121–134, 2008.

24. Lin, Z. and Q.-X. Chu, "A novel approach to the design of dual-band power divider with variable power dividing ratio based on coupled-lines," *Progress In Electromagnetics Research*, Vol. 103, 271–284, 2010.

25. Li, B., X. Wu, N. Yang, and W. Wu, "Dual-band equal/unequal Wilkinson power dividers based on coupled-line section with short-circuited stub," *Progress In Electromagnetics Research*, Vol. 111, 163–178, 2011.

26. Xi, L. and Y. Lin, "A novel design of dual-band Wilkinson power divider with simple structure and wide band-ratios characteristics," *Journal of Electromagnetic Waves and Applications*, Vol. 28, No. 13, 1635–1641, 2014.

27. Bedar Khan, Z., H. Zhao, and Y. Zhang, "Simplified approach for design of dual-band Wilkinson power divider with three transmission line sections," *Microwave and Optical Technology Letters*, Vol. 58, No. 10, 2374–2377, 2016.

28. Park, M.-J. and B. Lee, "A dual-band Wilkinson power divider," *IEEE Microwave and Wireless Components Letters*, Vol. 18, No. 2, 85–87, 2008.

29. Wu, Y., Y. Liu, S. Li, et al., "A new design method for unequal dual-band modified Wilkinson power divider," *Electromagnetics*, Vol. 30, No. 3, 269–284, 2010.

30. Wu, Y., Y. Liu, S. Li, et al., "Extremely unequal Wilkinson power divider with dual transmission lines," *Electronics Letters*, Vol. 46, No. 1, 90–91, 2010.

31. Al Shamaileh, K., N. Dib, and S. Abushamleh, "A dual-band 1: 10 Wilkinson power divider based on multi-T-section characterization of high-impedance transmission lines," *IEEE Microwave and Wireless Components Letters*, Vol. 27, No. 10, 897–899, 2017.

32. Li, X., Y.-J. Yang, L. Yang, S.-X. Gong, X. Tao, Y. Gao, K. Ma, and X.-L. Liu, "A novel design of dual-band unequal Wilkinson power divider," *Progress In Electromagnetics Research C*, Vol. 12, 93–100, 2010.

33. Salimi, P., "A design procedure for multi-section micro-strip Wilkinson power divider with arbitrary dividing ratio," *International Journal of New Technology and Research*, Vol. 3, No. 12, 263170, 2017.

34. Mongia, R., I. J. Bahl, and P. Bhartia, *RF and Microwave Coupled-line Circuits*, No Title, 1999.